Supplementary material for

Protein Arcs May Form Stable Pores in Lipid Membranes

Lidia Prieto, Yi He, Themis Lazaridis*

Department of Chemistry,
City College of New York,
160 Convent Ave,
New York, NY 10031

* Corresponding author. Tel. (212) 650-8364 fax (212) 650-6107
Email: tlazaridis@ccny.cuny.edu

Implicit simulations of protegrin self-assembly

We have run simulations of protegrin self-assembly using the implicit membrane model IMM1 (1), an extension of the EEF1 implicit solvation model of water-soluble proteins (2). In IMM1 the solvation parameters are expressed as a linear combination of those in water and in the membrane (represented by cyclohexane), weighed according to the position of the atoms along the *z*-axis (the membrane normal). Dielectric screening also changes depending on the z coordinate to account for strengthening of electrostatic interactions in the membrane. IMM1 has been extended to include anionic surface charge (3), transmembrane voltage (4), dipole potential (5), and lateral pressure (6). In this work we apply a modification that allows for membrane pores (7, 8) in which the solvation free energy becomes a function not only of the *z* coordinate of the atoms, but also of their distance r from the z axis. Both cylindrical and toroidal pores can be studied by making the pore radius a function of *z*: $R=R_o+kz'^2$, where z'=z/(T/2), R_o is the radius at z=0 and k is the curvature of the pore (0 for cylindrical pores).

The sequence of protegrin is RGGRLCYCRRRFCVCVGR-NH2, with at +7 net charge. In previous work (9) we showed that, both in implicit and explicit simulations of protegrin beta barrels, the most stable arrangement for the protegrin barrel is an NCNC parallel (NCNCpar) arrangement of the protegrin hairpins. This structure was shown to be more stable than the NCCN parallel (NCCNpar) and NCCN antiparallel (NCCNanti) arrangements. Here we test the ability of the peptides to self-assemble starting from non-interacting positions within the pore. Four peptides at the NMR structure (10) (PDB code 1PG1) were placed parallel to the membrane normal at the interface of a 13 Å, k=15 Å toroidal pore at 90° intervals and a 1 ns simulation was run. Different starting orientations were tried, so that lateral association of the peptides would produce NCCNpar, NCCNanti, and NCNCpar topologies.

When placed in an NCCNpar orientation the peptides moved out of the pore. For the remaining two topologies the peptides remained within the pore and associated.

For the NCNCpar arrangement the peptides assembled into an arc on one side of the pore (Fig. 1 in main text). In the NCCNanti topology the peptides also associated but did not line the pore and did not produce a continuous beta sheet (Fig. S1A). In addition, this oligomer has higher energy and less favorable transfer energy to the pore than the NCNCpar tetramer (Table S1). In fact, upon continuation of the simulation for a 2nd ns it starts to move out of the pore, whereas the NCNCpar tetramer remains in the pore. When 6 peptides were placed in an NCNCpar arrangement in the same pore, a broken beta sheet was observed with one of the hairpins near the center of the pore (Fig. S1B).

Table S1. Energies (kcal/mol) of self-assembled tetramers in a toroidal pore (R_0=13 Å, *k*=15 Å). <W> is the average effective energy and <ΔWtr> is the average transfer energy, calculated as <ΔWtr>=<Wmem-Wwater>. Averages are calculated over the last 0.6 ns of each simulation.

	<W>	**<ΔWtr>**
NCNCpar	-1671 ± 5	-13 ± 1
NCCNanti	-1641 ± 8	-6 ± 3

The NCNCpar tetramer arc was also simulated in an anionic membrane pore using an extension of IMM1 that employs a numerical solution of the Poisson-Boltzmann equation (11). The membrane had a thickness of 26 Å and anionic lipid fraction of 0.3. The pore was toroidal with radius R=13 Å, curvature K=15 Å, and relative headgroup density at the center h=0.6. The peptide tetramer was aligned with the pore so that its axis coincided with the pore axis. Four 3-ns simulations were carried out with different initial random velocities. The peptide center of mass was initially constrained to be between +/- 6.5 Å. Then the constraint was removed and the simulations were continued for another 3 ns. The transfer energy was obtained from the average of the four simulations. The final conformations are shown in figure S2. The same tetramer was also simulated on the planar membrane. The energies are given in Table S2.

Table S2. Energy (kcal/mol) of a tetramer in a 30% anionic toroidal pore (R_0=13 Å, *k*=15 Å, h=0.6) and on the planar membrane. <W> is the average effective energy and <ΔWtr> is the average transfer energy, calculated as <ΔWtr>=<Wmem-Wwater>.

	Planar mem	**Pore**	**Diff**
<W>	-1774 ± 11	-1786 ± 7	-12 ± 13
<ΔWtr>	-28.7 ± 0.3	-42.6 ± 0.8	-13.9 ± 0.9

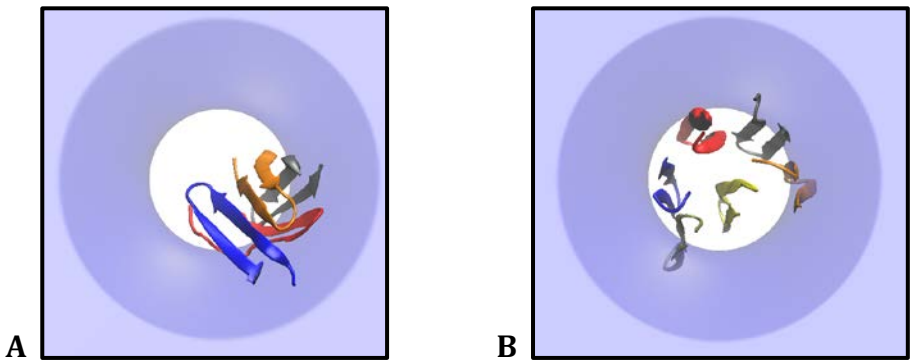

Figure S1. Upper views of the resulting structures from implicit simulations of the self-assembly of non-interacting protegrin monomers in a toroidal pore (R_0=13 Å and *k*=15 Å). **A.** 4 protegrin monomers arranged in an NCCNanti topology. **B.** 6 protegrin monomers in NCNCpar topology.

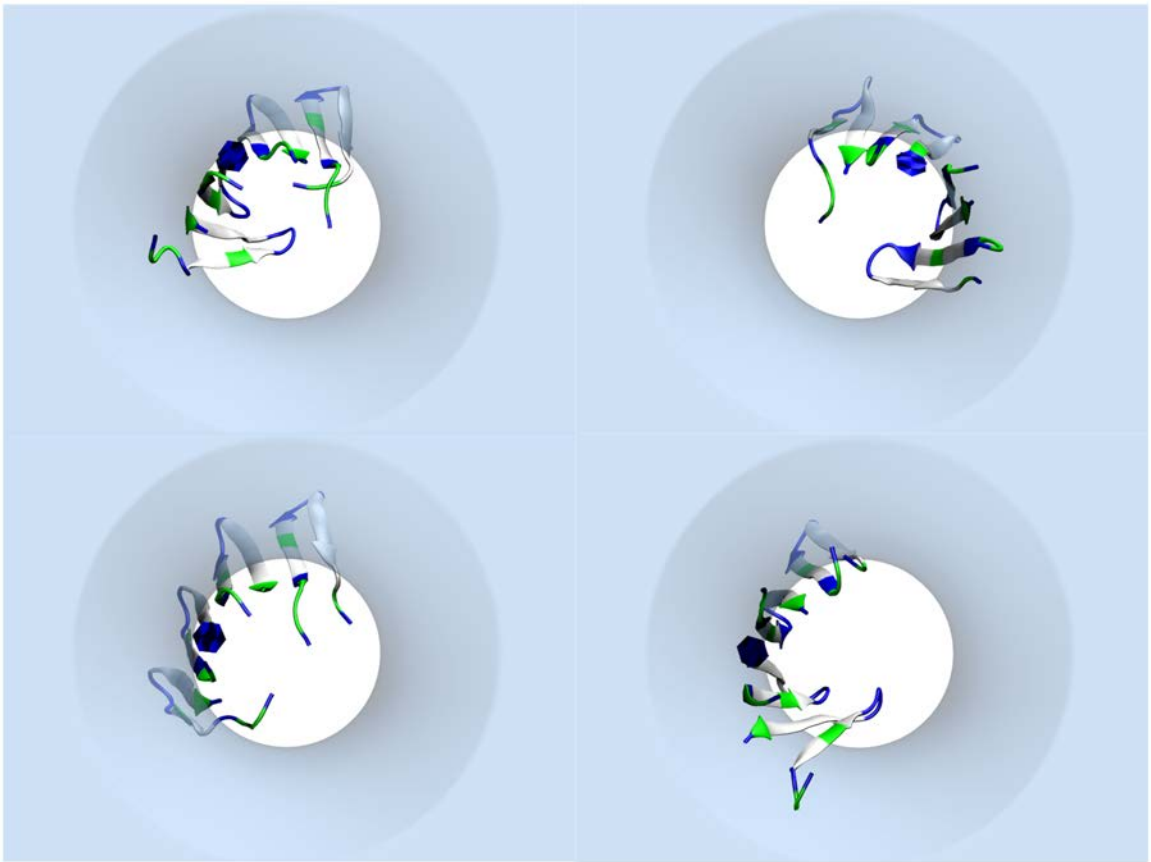

Figure S2. Upper views of the resulting structures from four independent simulations of the protegrin tetramer arc in a 30% anionic toroidal pore (R_0=13 Å, *k*=15 Å, h=0.6).

Table S3. Minimum distance between the Cζ atoms in the Arginine residues indicated (see Figure 4 in the main text) and the lipid head-group P atoms lining the non-protein part of the pore ($|z| \leq 8.5$Å) or the ones on the membrane surface ($|z| > 8.5$ Å). These values are averages over the last 100 ns. Red, grey, orange and blue are the colors of the monomers in main text Fig. 1. In bold are the distances highlighted in Fig. 4.

A. 100% POPC membrane

		RED	**GREY**	**ORANGE**	**BLUE**
P-Cζ1	*Pore*	**7 ± 2**	13 ± 3	20 ± 6	**8 ± 2**
	Surface	6 ± 2	6 ± 1	4.4 ± 0.3	8 ± 2
P-Cζ4	*Pore*	**4.9 ± 0.2**	10.3 ± 0.8	9.3 ± 0.7	**6 ± 2**
	Surface	11 ± 1	9 ± 1	12 ± 1	12 ± 2
P-Cζ10	*Pore*	20 ± 3	19 ± 2	19 ± 2	19 ± 3
	Surface	8 ± 2	12 ± 2	11 ± 1	4.4 ± 0.5

B. 70% POPE: 30% POPG membrane.

		RED	**GREY**	**ORANGE**	**BLUE**
P-Cζ1	*Pore*	26 ± 4	22 ± 3	10 ± 3	12 ± 4
	Surface	4.4 ± 0.3	6 ± 1	8 ± 2	5 ± 2
P-Cζ4	*Pore*	22 ± 3	18 ± 2	12 ± 2	**4.9 ± 0.7**
	Surface	8 ± 1	8.4 ± 0.6	11 ± 1	10 ± 1
P-Cζ10	*Pore*	**5 ± 1**	**8 ± 2**	17 ± 3	20 ± 2
	Surface	9 ± 2	5 ± 1	4.5 ± 0.4	4.6 ± 0.2

Figure S3. Distribution of the number of water molecules inside the pore (|z|< 8.5 Å). Green line: octameric protegrin rings inserted in preformed cylindrical pores (29). Red line: tetrameric arc inserted in preformed cylindrical pores. Black line: the same arc inserted in the membrane without a pore.

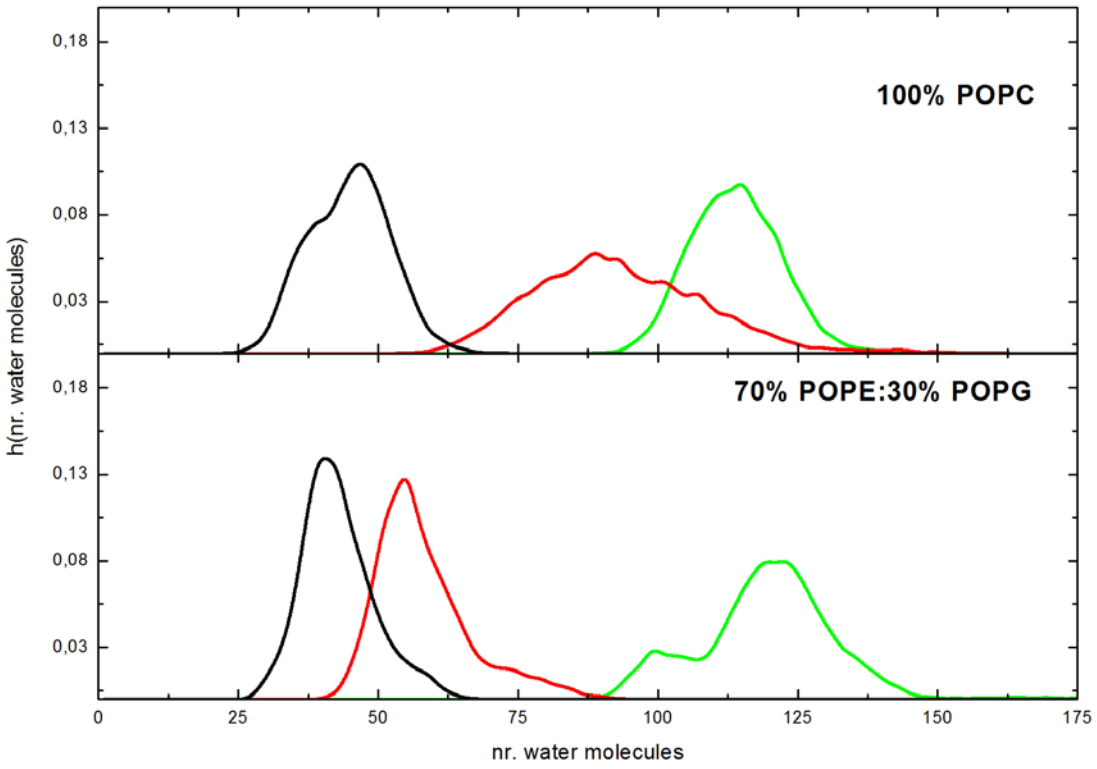

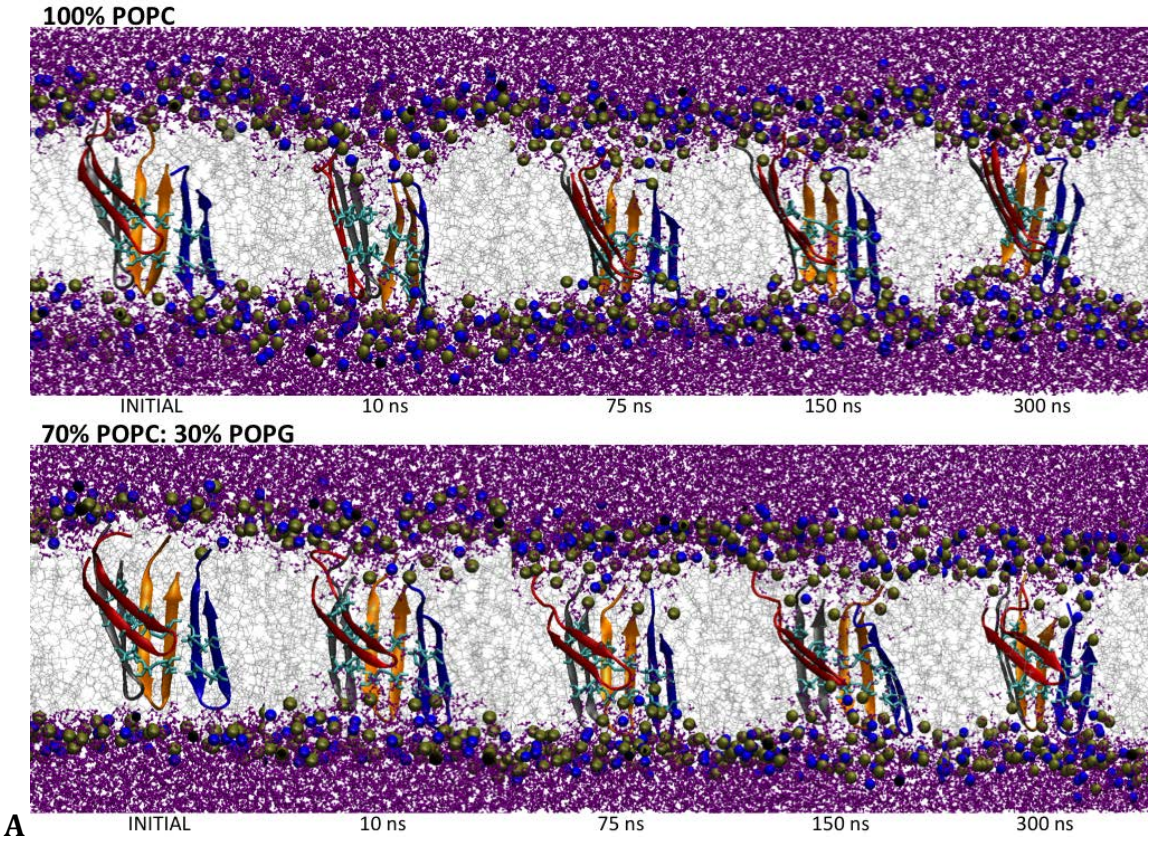

A

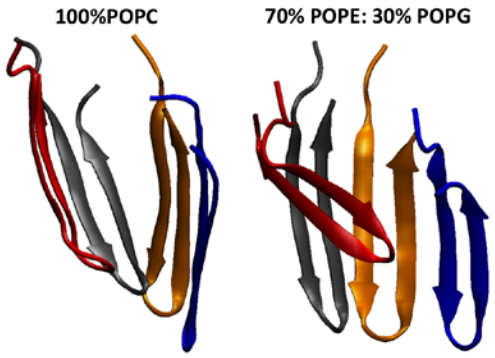

B

Figure S4. Arc pore structures in the membranes starting without a preformed pore. **A.** Snapshots along the simulations. The INITIAL structures correspond to the ones right before releasing all constraints. Purple balls-and-sticks: water molecules. Silver lines: lipid side-chains. Blue and tan spheres: lipid head group nitrogen and phosphorus atoms, respectively. Cyan licorice: disulphide bridges. Cartoon representations: peptide backbone. **B.** Structure at 300 ns of the arc peptide in the membrane (same as in A at 300 ns, eliminating membrane, water, and residue side chains). Figure made using VMD (12).

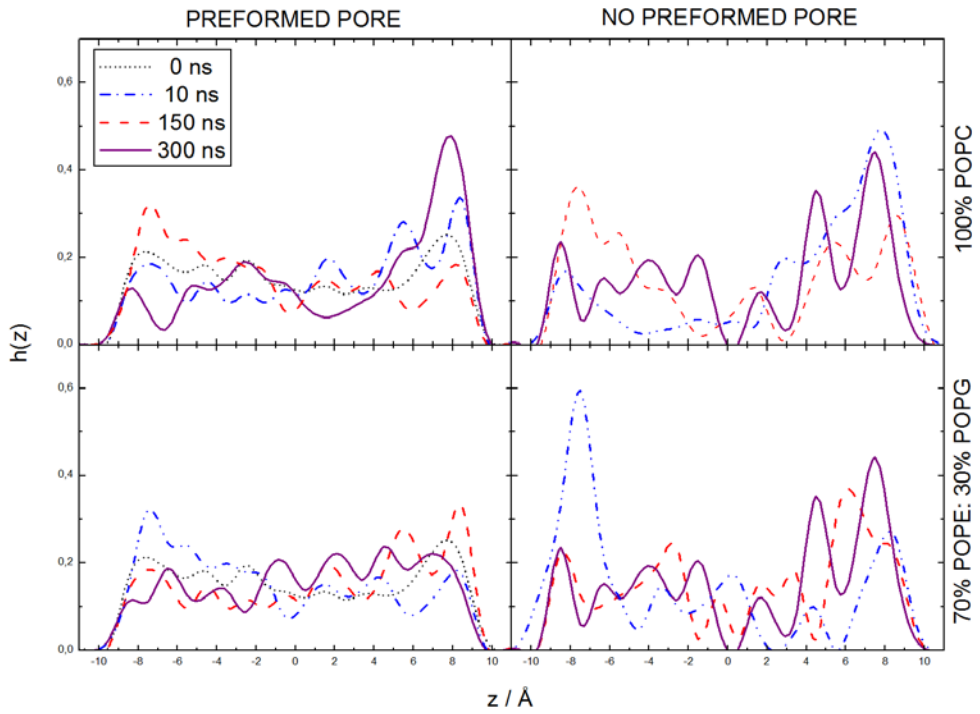

Figure S5. Distribution of water inside the pore ($|z| \leq 8.5$ Å).

Figure S6. Radius of the pore along the membrane normal (*z* axis) for the arcs in the membranes with preformed pores after 300-ns simulations. The water inside the pores (|z|< 8.5 Å) is also shown with VMD-surface representation mode (the upper part of the graph shows the pore in the POPC membrane, lower part of the graph shows the pore in the POPE:POPG membrane). The radius was estimated as follows: the pore region (|z|<8.5) was divided in 0.5 Å slices and the number of water molecules in them was calculated, which allows calculation of the volume. Modeling these volumes as small cylinders, we can calculate the radius of the pore at that specific point.

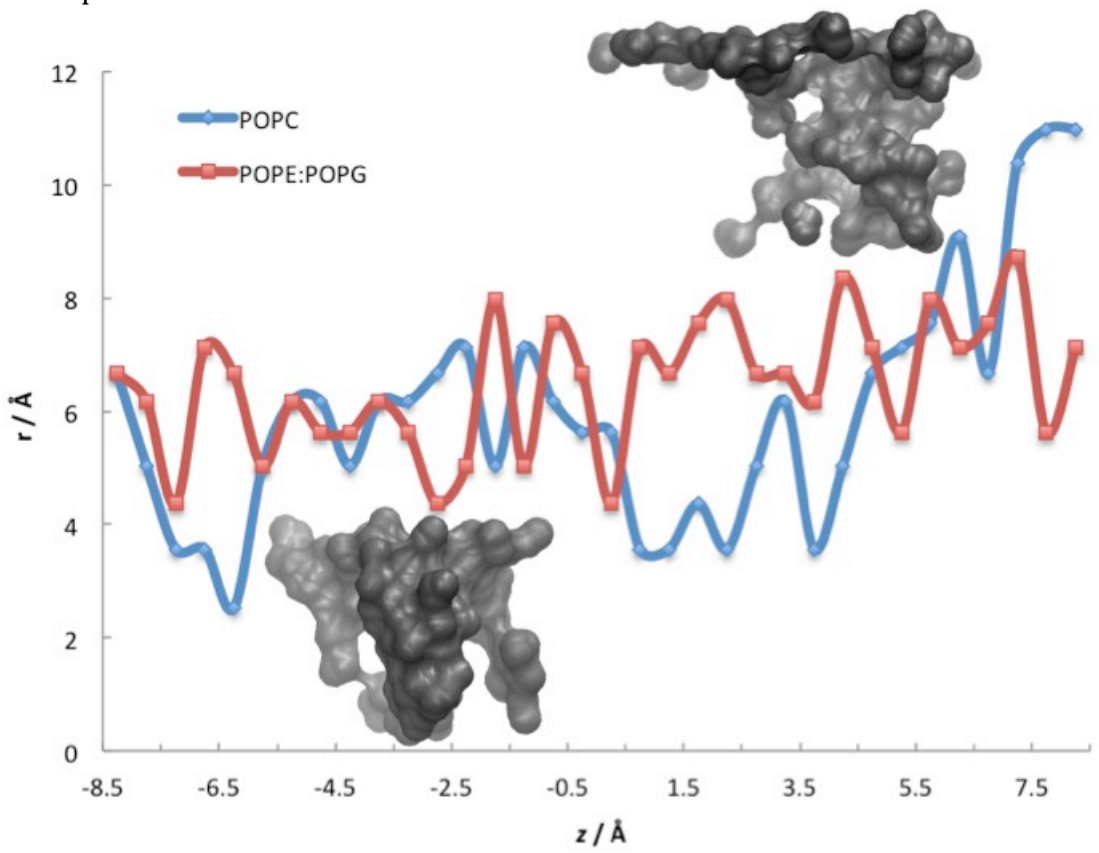

Figure S7. Distribution of the position along the z axis with respect to the membrane center of the center of mass of the arcs in the simulations. The average positions are -5 ± 1 Å (initially -2.8) for POPC, -3 ± 2 Å (initially -2.7) for POPC no pore, 1 ± 1 Å (initially -0.23) for PE/PG, and -2 ± 1 Å (initially -0.04) for PE/PG no pore.

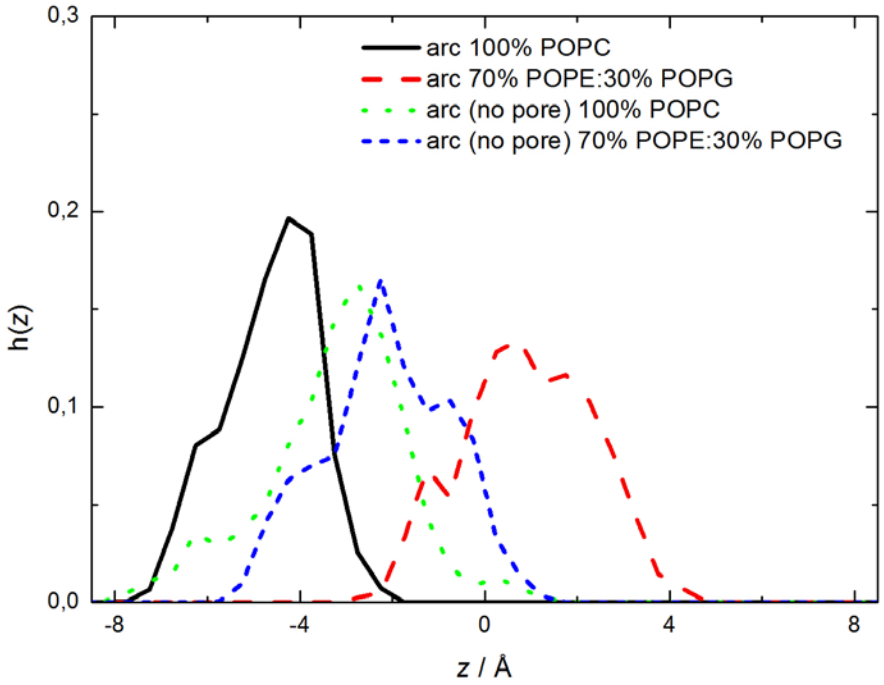

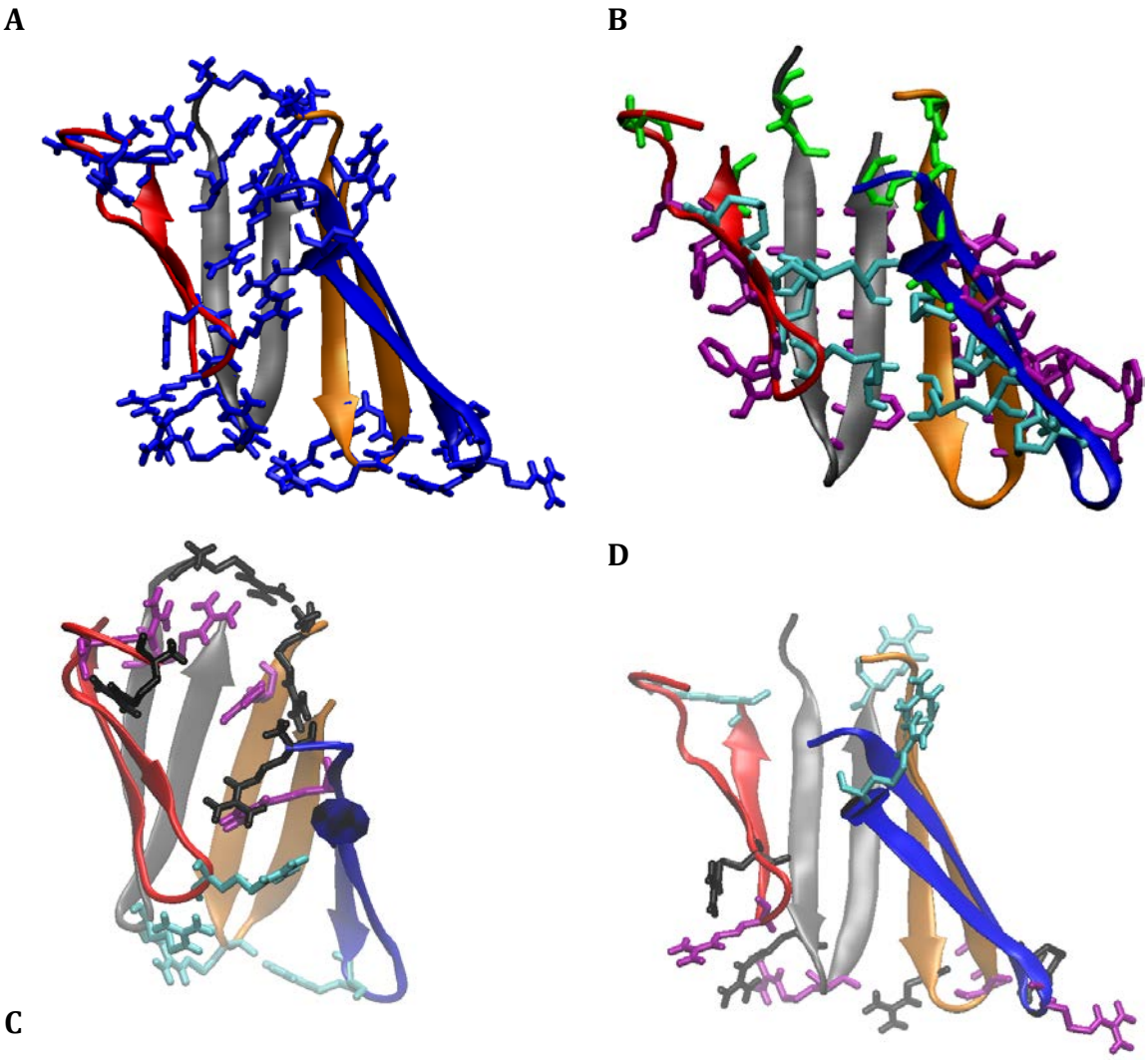

Figure S8. Residue distribution in the arc structure used as initial structure in our simulations (Figure 1 of the main text). **Upper panel**: Distribution of charged (A) and neutral (B) residues in the initial arc structure (Blue - positively charged, green - polar neutral, purple – hydrophobic, cyan – Cysteine disulfide bonds). **Lower panel**: Position in the initial arc structure of ARG residues pointing C) towards the pore (Black – ARG1, purple – ARG4, and cyan - ARG10, D) towards the membrane (Black – ARG9, purple – ARG11, and cyan – ARG18) in the initial arc structure.

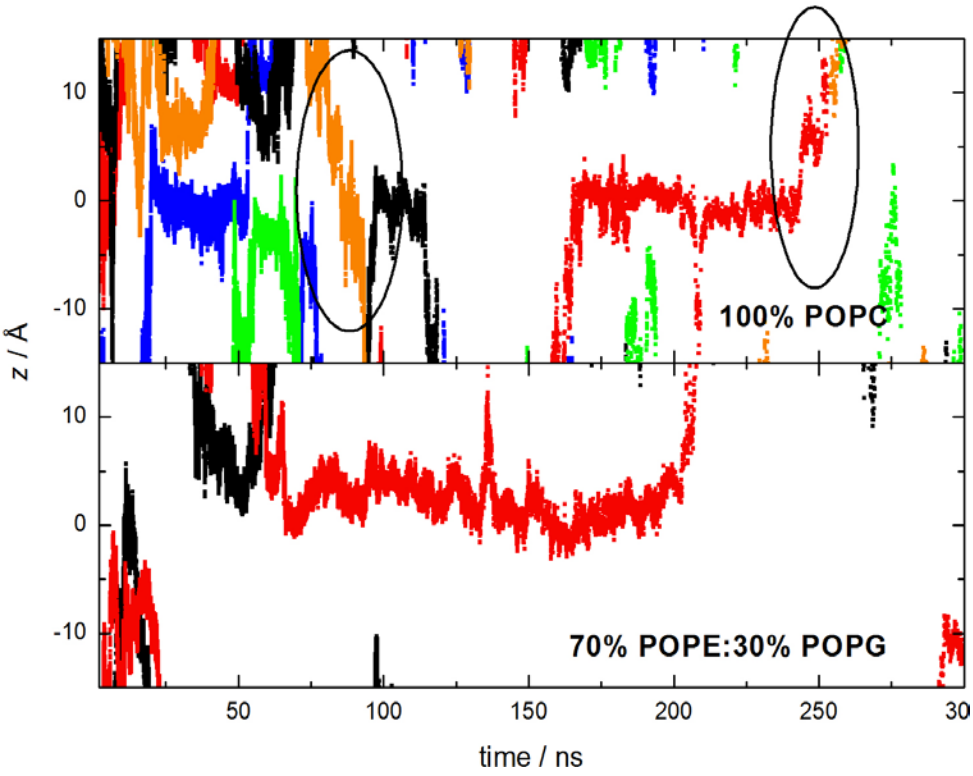

Figure S9. z coordinate of some of the Cl^- ions entering the pore region ($|z| \leq 8.5$ Å). The circles highlight membrane-crossing events. In some cases the ions appear on one side and the other of the membrane without crossing the membrane center, due to the periodic boundary conditions.

Supporting References

1. Lazaridis T (2003) Effective energy function for proteins in lipid membranes. *Proteins-Structure Function and Genetics* 52(2):176-192.
2. Lazaridis T & Karplus M (1999) Effective energy function for proteins in solution. *Proteins* 35(2):133-152.
3. Lazaridis T (2005) Implicit solvent simulations of peptide interactions with anionic lipid membranes. *Proteins* 58(3):518-527.
4. Mottamal M & Lazaridis T (2006) Voltage-dependent energetics of alamethicin monomers in the membrane. *Biophysical Chemistry* 122(1):50-57.
5. Zhan H & Lazaridis T (2012) Influence of membrane dipole potential on peptide binding to lipid bilayers. *Biophysical Chemistry* 161:1-7.
6. Zhan H & Lazaridis T (2013) Inclusion of Lateral Pressure/Curvature Stress Effects in Implicit Membrane Models. *Biophysical Journal* 104(3):643-654.
7. Lazaridis T (2005) Structural determinants of transmembrane beta-barrels. *Journal of Chemical Theory and Computation* 1(4):716-722.
8. Mihajlovic M & Lazaridis T (2010) Antimicrobial peptides bind more strongly to membrane pores. *Biochimica Et Biophysica Acta-Biomembranes* 1798(8):1494-1502.
9. Lazaridis T, He Y, & Prieto L (2013) Membrane Interactions and Pore Formation by the Antimicrobial Peptide Protegrin. *Biophysical Journal* 104(3):633-642.
10. Fahrner RL*, et al.* (1996) Solution structure of protegrin-1, a broad-spectrum antimicrobial peptide from porcine leukocytes. *Chemistry & Biology* 3(7):543-550.
11. He Y, Prieto L, & Lazaridis T (2013) Modeling peptide binding to anionic membrane pores. *J Comput Chem* 34:1463-1475.
12. Humphrey W, Dalke A, & Schulten K (1996) VMD: Visual molecular dynamics. *Journal of Molecular Graphics & Modelling* 14(1):33-38.